Available online at www.sciencedirect.com
ScienceDirect
International Journal of Thermal Sciences 46 (2007) 1242–1250
International Journal of Thermal Sciences
www.elsevier.com/locate/ijts

# Experimental study of forced convection in metallic porous block subject to a confined slot jet

Tzer-Ming Jeng [a,*], Sheng-Chung Tzeng [b]

[a] *Department of Mechanical Engineering, Air Force Institute of Technology, Gangshan 820, Taiwan, ROC*
[b] *Department of Mechanical Engineering, Chienkuo Technology University, Changhua 500, Taiwan, ROC*

Received 21 August 2006; received in revised form 29 November 2006; accepted 3 January 2007

Available online 20 February 2007

**Abstract**

This study experimentally investigated the convective heat transfer and pressure drop in the metallic porous block with a confined slot air jet. Aluminum foam block with the porosity of 0.93 and the pore density of 10 *PPI* (pores per inch) was used. The size of the aluminum foam block was fixed. Variable parameters were the ratio of the jet nozzle width to the porous block height ($W_j/H$), the ratio of the jet-to-foam tip distance to the porous block height ($C/H$) and the jet Reynolds number ($Re$). Experimental results reveal that the wall temperature at the stagnation point ($x/L = 0$) under the slot jet flow was minimal, and monotonously rise along the channel axis until the channel exit. Parametric studies indicate that increasing $Re$ increased the average Nusselt number ($Nu$), decreasing $W_j/H$ slightly increased $Nu$, and the effect of $C/H$ on $Nu$ were negligible. The dimensionless pressure drop ($C_f Re^2 (L/W_j)^2$) increased as $Re$ increased or $W_j/H$ declined. The effect of $C/H$ on $C_f Re^2 (L/W_j)^2$ does not seem regular. Besides, The $Nu$ in the configuration without by-pass flow (i.e. $C/H = 0$) generally exceeded that with by-pass flow (i.e. $C/H = 1$–3) at a given dimensionless pumping power ($C_f Re^3 (L/W_j)^2$). Within the successfully measured parameter ($W_j/H = 0.22$–$0.35$, $C/H = 0$–3 and $Re = 1697$–$31\,003$), the largest $Nu$ under the same $C_f Re^3 (L/W_j)^2$ appeared on $W_j/H = 0.35$ and $C/H = 0$.


*Keywords:* Heat transfer; Pressure drop; Metallic porous block; Slot jet; Experiments

## 1. Introduction

Jet impingement is a high-performance technique for cooling a local surface area. Its applications in industries where severe heat dissipation are popular, such as annealing metals, tempering glass, drying paper and textiles, and cooling of gas turbine blades and electronics equipment. Therefore, the heat transfer of jet impingement onto a plate has attracted considerable attention [1–6]. To further improvement of cooling technology of jet impingement, several studies [7–12] have reported the potential of combining extended surfaces with impinging jets. The heat transfer is enhanced by the extended surface due to the increase of the heat dissipation area and the flow mixing. Recently, Issa and Ortega [13] experimentally measured the pressure drop and heat transfer of a square jet impinging onto the square pin-fin heat sink. Their conclusions in the aspect of the heat transfer indicated that the overall thermal resistance decreased with increasing pin density or pin diameter. The effect of pin-fin height on the thermal resistance was weak. Moreover, short pin-fins at low Reynolds number were most strongly sensitive to variations in tip clearance. Lin et al. [14] experimentally investigated the cooling performance from the plate-fin heat sinks with a confined slot jet impingement. They proposed a complete composite correlation of steady-state average Nusselt number for mixed convection due to jet impingement and buoyancy. All above studies addressed the cooling of impinging jet onto the finned heat sinks.

Besides the finned heat sink, the metallic porous material has been proven that is a good extended surface in heat dissipation of cross flow [15–20]. Some studies of combining porous material and jet impingement have been also reported. Fu and Huang [21] numerically studied the thermal performance of

* Corresponding author. Tel.: +886 7 6256040; fax: +886 4 7357193.
*E-mail addresses:* tm.jeng@msa.hinet.net, t_m_jeng@yahoo.com.tw (T.-M. Jeng).

1290-0729/$ – see front matter 
doi:10.1016/j.ijthermalsci.2007.01.007

**Nomenclature**

| | | | |
|---|---|---|---|
| $C$ | jet-to-foam tip distance | m | |
| $C_f$ | friction factor, $(p_j - p_e)/(0.5\rho_f V_j^2)$ | | |
| $Da$ | Darcy number, $K/H^2$ | | |
| $F$ | inertial coefficient | | |
| $H$ | height of the aluminum foam block | m | |
| $H_c$ | height of the test channel | m | |
| $h_v$ | volumetric heat transfer coefficient | $W/m^3/°C$ | |
| $K$ | permeability | $m^2$ | |
| $k$ | thermal conductivity | $W/m/°C$ | |
| $L$ | length of the aluminum foam block | m | |
| $Nu$ | average Nusselt number, Eq. (3) | | |
| $Nu_{fs}$ | fluid-to-solid Nusselt number, $h_v H^2/k_f$ | | |
| $p$ | pressure | Pa | |
| $PPI$ | pore density of the aluminum foam block, pores per inch | | |
| $q_c$ | convective heat flux | $W/m^2$ | |
| $q_k$ | conductive heat loss | $W/m^2$ | |
| $q_r$ | radiative heat loss | $W/m^2$ | |
| $q_t$ | total heat flux generated by the thermofoil heater | $W/m^2$ | |
| $Re$ | jet Reynolds number, $\rho_f V_j W_j/\mu$ | | |
| $s$ | spacing between thermocouples | m | |
| $T$ | temperature | °C | |
| $U_e$ | average fluid velocity at the channel exit | m/s | |
| $V_j$ | average fluid velocity at the jet nozzle | m/s | |
| $W$ | width of the aluminum foam block or the test channel | m | |
| $W_j$ | the jet nozzle width | m | |
| $x$ | axial coordinate | m | |

*Greek symbols*

| | | |
|---|---|---|
| $\varepsilon$ | porosity | |
| $\mu$ | viscosity | kg/m/s |
| $\theta$ | dimensionless temperature, $(T - T_j)/(q_c L/k_f)$ | |
| $\rho$ | density | $kg/m^3$ |

*Superscripts*

| | |
|---|---|
| $*$ | effective |

*Subscripts*

| | |
|---|---|
| e | channel exit |
| f | fluid |
| j | jet nozzle |
| s | solid matrix |
| w | channel wall |

variously shaped porous blocks under a fully unconfined slot jet. They used the empirical formulas for the porous properties of a packed spherical bed to solve the momentum equation. They assumed that the fluid and porous medium is at local thermal equilibrium, and thus used the one-equation model to construct the energy equation. Their work revealed that the element that dominates the total performance of porous blocks is the amount of flow that nears the heated surface. Hadim and North [22] numerically investigated the forced convection in a sintered porous channel with inlet and outlet slots. They also used the one-equation model to construct the energy equation. Their work evaluated the effects of particle diameter, particle Reynolds number, channel height, and slot width on the Nusselt number and friction factor. The relevant correlations were proposed. Jeng and Tzeng [23] examined the heat transfer characteristics of porous heat sinks with a confined slot jet. Their results reveal that when the Reynolds number is low, the heat transfer was maximal at the stagnation point. However, as the Reynolds number increased, the maximum heat transfer moved downward to the narrowest part between the recirculation zone and the heating surface. Saeid and Mohamad [24] numerically investigated the mixed convection of porous media with a confined jet. The various parameters included Rayleigh number, Peclet number, jet width and the distance between the jet and the heated surface. They reported that the average Nusselt number increased with increasing Rayleigh number or jet width when Peclet number was high. Besides, narrowing the distance between the jet and the heated surface could increase the average Nusselt number.

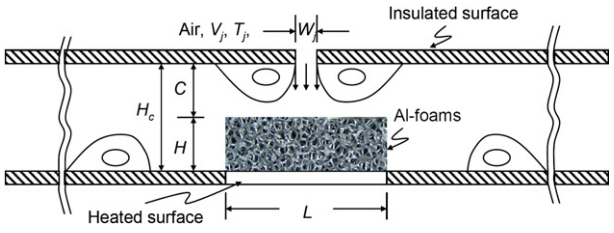


Fig. 1. Physical model.

All of the aforementioned work employed the numerical method to investigate the heat transfer of combining porous material and jet impingement. However, few experimental studies have addressed this issue. Fig. 1 presents the physical model of this study. Based on the fluid flow dynamics, a reasonable streamline pattern is also plotted in Fig. 1. When the jet is impinging the top surface of the porous block, some of fluid will flow over the top surface and other will flow into the interior of the porous block. A pair of vortex will appear next to the jet nozzle, and then the leakage flow over the top of the porous block will separate from the edge of the porous block to combine with the flow blowing from the porous block. Another pair of vortex will be generated at a far place in the downstream of the porous block. As for cooling of jet impingement, heat transfer is closely related to fluid flow. The flow field of an impinging jet onto a porous block is more complicated than that onto a smooth surface or a solid block. These results motivate this work.

This investigation addressed the convective heat transfer and pressure drops in metallic porous block with a confined

slot jet. Aluminum foam block with the porosity of 0.93 and the pore density of 10 *PPI* (pores per inch) was employed. The coolant was air. The size of the aluminum foam block was fixed. Variable parameters were the ratio of the jet nozzle width to the porous block height ($W_j/H$), the ratio of the jet-to-foam tip distance to the porous block height ($C/H$) and the jet Reynolds number ($Re$). Parametric studies on both the average Nusselt number ($Nu$) and the dimensionless pressure drop ($C_f Re^2 (L/W_j)^2$) were presented. Finally, based on the maximum $Nu$ at a given dimensionless pumping power ($C_f Re^3 (L/W_j)^2$), the optimal configuration of $W_j/H$ and $C/H$ in the present cooling system were suggested.

## 2. Experimental setup

### 2.1. Test section and apparatus

The experimental system, presented in Fig. 2, comprises three parts – a wind tunnel, a porous medium test section and a data acquisition system. The wind tunnel is made of 10 mm-thick Plexiglas plates. The main flow of air was supplied using a blowing machine, and the flow rate was controlled by using an inverter. After it passes through a straightening section, the flowing air normally impinges into the test channel from the slot entries of various widths. The test channel made of 40 mm-thick Bakelite plates has a rectangular cross section of 60 mm-width and various heights filled with 120 mm-long × 60 mm-width × 20 mm-height aluminum foam block. A thermofoil heater was attached to the inner surface of the bottom wall of the test channel. The other walls of the channel were insulated. Table 1 provides the porous characteristics

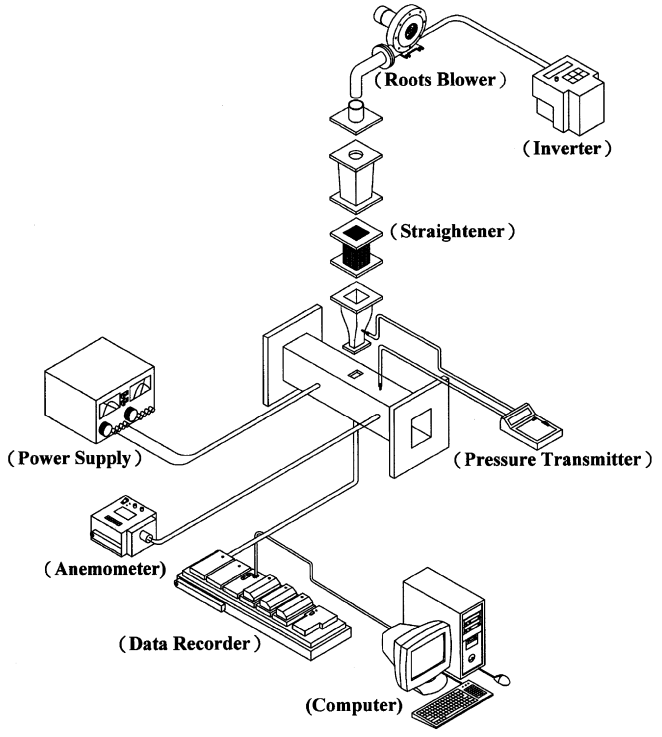


Fig. 2. Experimental setup.

Table 1
Characteristics of aluminum foam block used herein

| $L \times W \times H$ (cm) | $\varepsilon$ | $PPI$ | $F$ | $K$ ($\times 10^8$ m$^2$) | $k^*$ (W/m/°C) |
|---|---|---|---|---|---|
| 12 × 6 × 2 | 0.93 | 10 | 0.0476 | 23.4 | 5.23 |

of the aluminum foam block, such as the permeability ($K$), the inertial coefficient ($F$), the effective thermal conductivity ($k^*$), etc. The $K$ and $F$ values were determined by the method reported by Hunt and Tien [15]. The value of $k^*$ was measured by performing a number of one-dimensional conduction heat transfer experiments (the test method can be found in Ref. [25]). The aluminum foam block with the porosity ($\varepsilon$) of 0.93 and the pore density of 10 *PPI* (pores per inch) was brazed onto 3 mm-thick aluminum spreader (as shown in the close-up view in Fig. 3(a)). Seven 36-gauge T-type thermocouples were fixed to the bottom skin of the spreader along the channel axis, as displayed in Fig. 3(b). Seven other thermocouples were used to monitor the ambient temperature, the air temperature at the channel inlet and the air temperature at the channel exit. A total of 14 thermocouples were connected to the data logger. The system was assumed to be in a steady state when the temperature did not vary by over 0.2 °C during an interval of 15 minutes. An anemometer was installed in the rear section after the test section to measure the speed ($U_e$) of the airflow (see Fig. 2). We assume that the jet flow leaving slot nozzle normally impinge onto the aluminum foams, and then symmetrically enter into the right and left channels of the test section. So the average air velocity at the slot nozzle ($V_j$) can be expressed as $V_j = 2 \times U_e \times (H + C)/W_j$. Besides, a pressure transmitter was utilized to measure the pressure drop associated with the flow of air through the test section.

### 2.2. Data reduction and uncertainty analysis

The measured fluid velocities, temperatures and pressure drops were used to determine the dimensionless wall temperatures, the jet Reynolds numbers, the average Nusselt numbers and the friction factors, using

$$\theta_w = \frac{T_w - T_j}{q_c L/k_f} \tag{1}$$

$$Re = \frac{\rho_f V_j W_j}{\mu} \tag{2}$$

$$Nu = \frac{hL}{k_f} = \left( \sum_{i=1}^{7} \frac{1}{\theta_{w,i}} \right) s \Big/ \frac{L}{2} \tag{3}$$

$$C_f = \frac{p_j - p_e}{0.5 \rho_f V_j^2} \tag{4}$$

where $T_w$ is the temperature measured at the bottom skin of the aluminum foam block; $T_j$ is the air temperature at the slot nozzle; $k_f$ is the thermal conductivity of air based on the inlet air temperature (about 0.026 W/m/°C); $q_c$ represents the convective heat flux; $V_j$ represents the average air velocity at the slot nozzle; $s$ is the spacing between thermocouples; $L$ is the length of aluminum foam block, and $p_j$ and $p_e$ are the static pressures

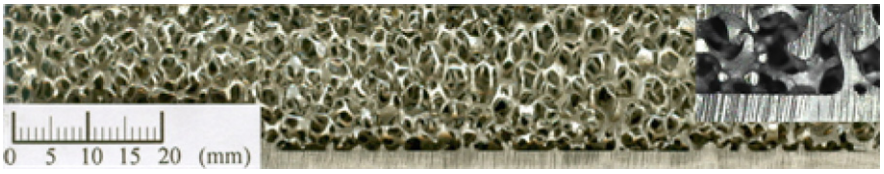


(a) Photo of Al-foams

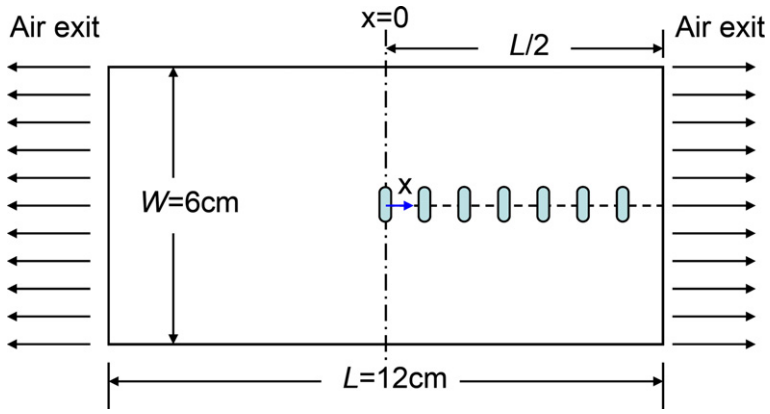


(b) Positions of thermocouples

Fig. 3. Photo of Al-foams and positions of thermocouples.

at the jet nozzle and the channel exit, respectively. Notably, the effective thermal conductivity ($k^*$) is important for the porous medium (Ref. [26]). The dimensionless temperature (as Eq. (1)) and the Nusselt number (as Eq. (3)) sometimes are defined in term of $k^*$ not $k_f$. Therefore, we also provide the $k^*$ value of the present aluminum foam block in Table 1 for the alternative.

The total heat flux ($q_t$) generated by the thermofoil heater may be transformed into three heat-transfer modes in the steady-state experiment to evaluate the convective heat flux dissipated from the heated surface, as determined by the conservation of energy. These modes are, (1) radiative heat loss, $q_r$; (2) conductive heat loss, $q_k$, and (3) convective heat dissipated from the heated surface, $q_c$. Accordingly

$$q_c = q_t - q_r - q_k \tag{5}$$

This energy-balance equation determines the net convective heat flux ($q_c$) from the heated surface to the flowing air in the channel. The total heat flux ($q_t$) is $V^2/R$. Herein, $V$ is the output voltage of the DC power supply and $R$ is the resistance of the thermofoil heater. The radiative heat loss ($q_r$) from the inlet and exit surfaces of aluminum foam to its surroundings, is obtained using thermally diffusive gray-body networks. The maximum radiative heat loss is under 2.1% of the total input heat flux herein. The conductive heat loss ($q_k$) to the insulated Bakelite is estimated using a two-dimensional conduction models. The $q_k$ values vary from 0.2% to 3.2% of the total input heat flux in the experiments. Hence, the convective heat dissipated from the heated surface ($q_c$) can be determined, and the dimensionless wall temperatures ($\theta_w$) and the average Nusselt numbers ($Nu$) finally calculated.

The standard single-sample uncertainty analysis, as recommended by Kline and McClintock [27] and Moffat [28], was performed. Data supplied by the manufacturer of the instrumentation stated that the measurement of flow velocity and pressure drop have a 1% error. The uncertainty in the measured temperature was ±0.2 °C. The experimental uncertainty in the convective heat flux ($q_c$) was estimated to be 2.4%. The experimental data herein reveal that the uncertainties in the jet Reynolds number, the friction factor and the average Nusselt number were 1.5%, 2.2% and 7.1%, respectively.

## 3. Results and discussion

The convective heat transfer, $Nu$, in the metallic porous block subject to a confined slot jet and isoflux heating on the bottom surface of the porous block (Fig. 1), is a function of several dimensionless parameters and is given by

$$Nu = fun.\left(\frac{L}{H}, \frac{W}{H}, \frac{W_j}{H}, \frac{C}{H}, Da, Nu_{fs}, Re\right) \tag{6}$$

where ($L \times W \times H$) is the size of the aluminum foam block and is constant herein; $W_j$ is the width of the perpendicular slot entry; $C$ is the jet-to-foam tip distance; $Da$ ($\equiv K/H^2$, where $K$ is the permeability and is dependent on the inner structure of the porous block) is the Darcy number; $Nu_{fs}$ ($\equiv h_v H^2/k_f$, where $h_v$ is the volumetric heat transfer coefficient and is dependent on the local flow velocity and the inner structure of the porous block) is the fluid-to-solid Nusselt number, and $Re$ is the jet Reynolds number. Therefore, Eq. (6) can be reduced to be

$$Nu = fun.\left(\frac{W_j}{H}, \frac{C}{H}, Nu_{fs}, Re\right) \tag{7}$$

Herein, $W_j$, $C$ and the mass flow rate are variable and influence the values of $Nu_{fs}$ in the present system due to the various flow patterns. In other words, the $Nu_{fs}$ is dependent on $W_j$, $C$ and the mass flow rate in the present study since the inner structure of the porous block is fixed. Therefore, the results and discussion would ignore the effect of the $Nu_{fs}$ ($\equiv h_v H^2/k_f$).

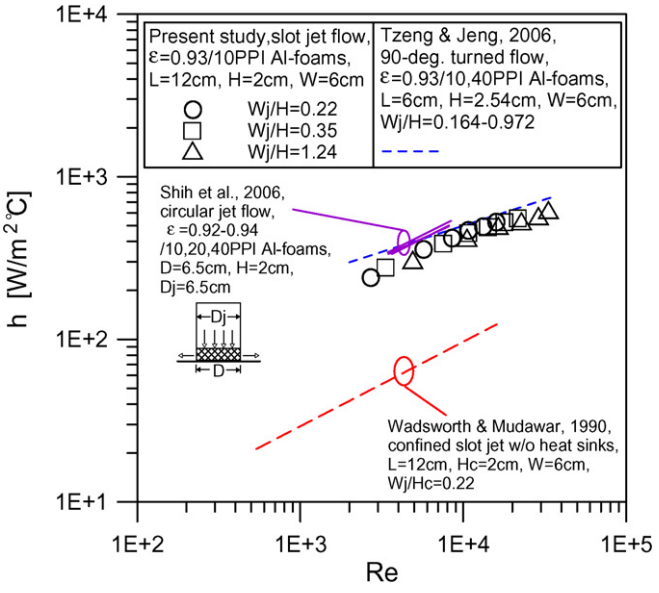


Fig. 4. Comparison of present results with data of 90-deg. turned flow system ($C = 0$).

Additionally, one can find the details about the measurement of the volumetric heat transfer coefficient ($h_v$) in the study of Calmidi, R.L. Mahajan [16]. As for cooling of jet impingement, heat transfer is closely related to fluid flow. Theoretically, if more air is flown into the porous block, the cooling performance will be better. The variables that affect the amount of air going inside the porous block herein include the velocity of jet flow, the nozzle-to-foam tip distance and the width of the slot nozzle. However, it is worth noting that the aluminum foam block used in this study has homogenous and isentropic characteristics, and its effective thermal conductivity is relatively large. Therefore, when the amount of air going inside the porous block decreases, the heat flux from the heated surface can be conducted to the outside of the aluminum foam block effectively via conduction, and then transfer to by-pass air via convection. Therefore, in terms of heat transfer of aluminum foam block, whether the air goes inside the heat sink may become uncertain. In this investigation, $W_j/H$ are 0.22–1.24; $C/H$ varies from 0 to 3, and $Re$ varies from 1697 to 33 314. A series of experiments are conducted to elucidate the effects of $W_j/H$, $C/H$ and $Re$ on the convective heat transfer in an aluminum foam block subject to a confined slot jet.

The experimental data concerning the heat transfer characteristics in porous block with a slot impinging jet are lacking, so the validity of the experiments conducted herein is established by comparing with the data obtained by Tzeng and Jeng [29] in an aluminum foam channel with 90-deg turned flow. Tzeng and Jeng [29] proposed the correlation for the average Nusselt number as

$$\frac{hL}{k_f} = 71.88\left(\frac{\rho_f U_e H}{\mu}\right)^{0.322} \tag{8}$$

where $U_e$ is the average fluid velocity at the channel exit. The range of application of Eq. (8) is $W_j/H = 0.164$–$0.972$ and $\rho_f U_e H/\mu = 1376$–$23\,619$, for $\varepsilon = 0.93/10$ *PPI* aluminum foams and $(L \times W \times H) = (6\text{ cm} \times 6\text{ cm} \times 2.54\text{ cm})$. The cooling system studied by Tzeng and Jeng [29] was similar with the half of the present impinging system. Additionally, the recently experimental data of Shih et al. [30] for circular jet flow onto an aluminum foam cylinder are also employed for comparison. Fig. 4 presents the results of the comparison and demonstrates that the measurements herein are reasonable. Moreover,

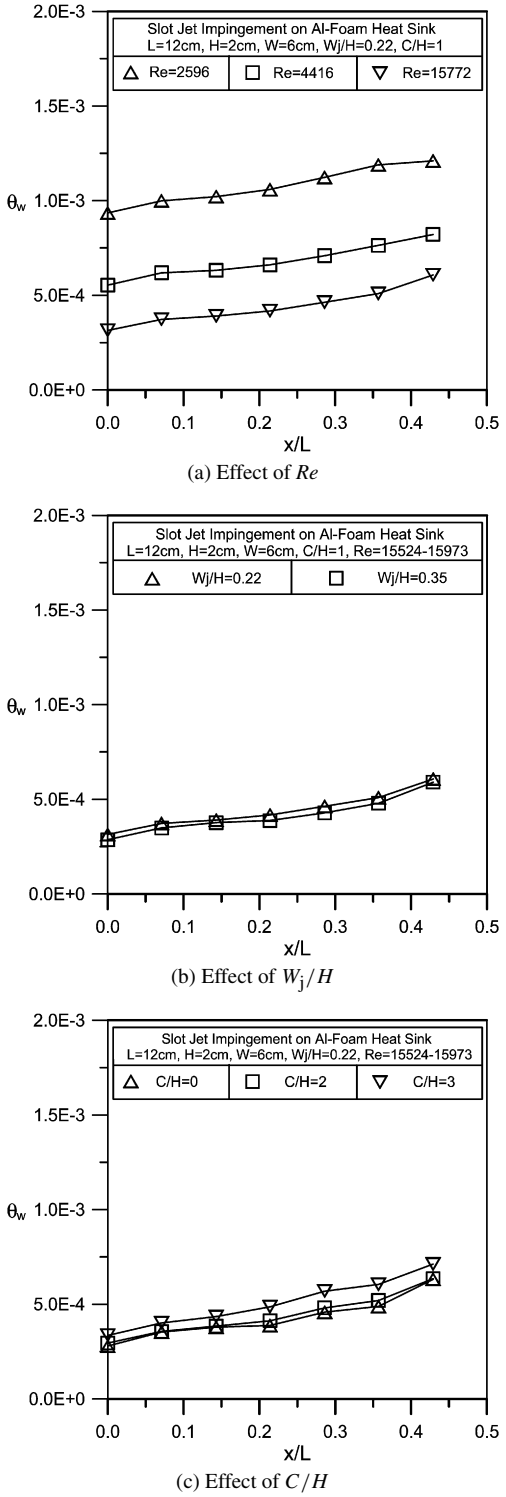


Fig. 5. Dimensionless wall temperature distributions along the channel axis.

Table 2
Coefficients of the correlations between $Nu$ and $Re$

| $\varepsilon = 0.93/10$ *PPI* Al-foams $L \times W \times H$ cm $= 12 \times 6 \times 2$ | | $Nu = m_1 Re^{n_1}$ | | | |
|---|---|---|---|---|---|
| $W_j/H$ | $C/H$ | $Re$ | $m_1$ | $n_1$ | Standard error |
| 0.22 | 0 | 2710–15 973 | 33.125 | 0.444 | 1.096E–3 |
| 0.22 | 1 | 2596–15 772 | 25.939 | 0.469 | 7.894E–3 |
| 0.22 | 2 | 1697–15 760 | 43.542 | 0.415 | 2.001E–3 |
| 0.22 | 3 | 3262–15 524 | 41.488 | 0.402 | 0.265E–3 |
| 0.35 | 0 | 3333–21 622 | 60.12 | 0.375 | 0.527E–3 |
| 0.35 | 1 | 3657–19 825 | 28.451 | 0.454 | 2.803E–3 |
| 0.35 | 2 | 1774–17 993 | 48.197 | 0.386 | 1.171E–3 |
| 0.35 | 3 | 3903–31 003 | 114.079 | 0.292 | 0.718E–3 |

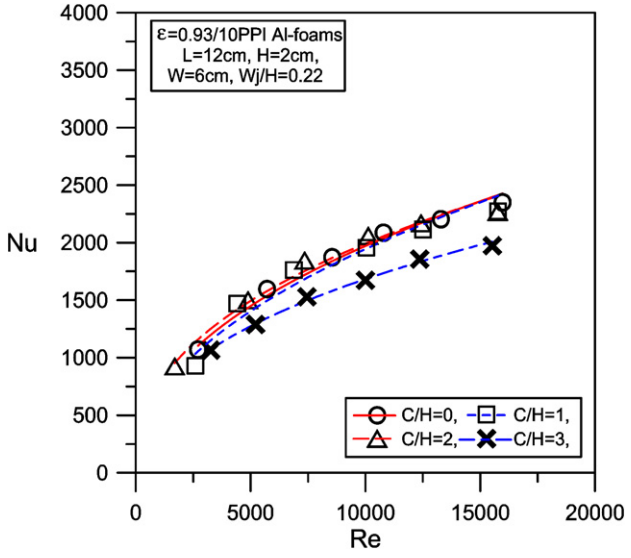


(a) $W_j/H = 0.22$

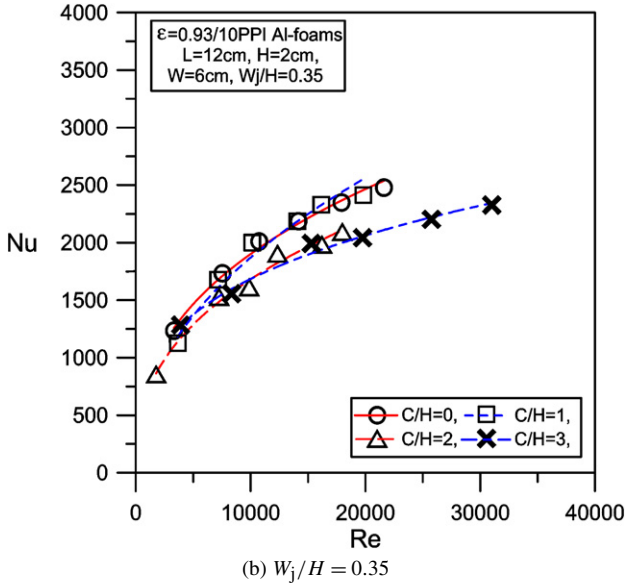


(b) $W_j/H = 0.35$

Fig. 6. Nusselt number as a function of jet Reynolds number.

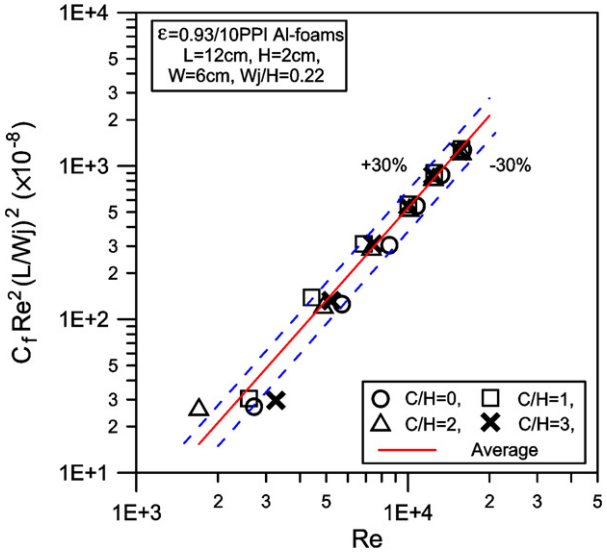


(a) $W_j/H = 0.22$

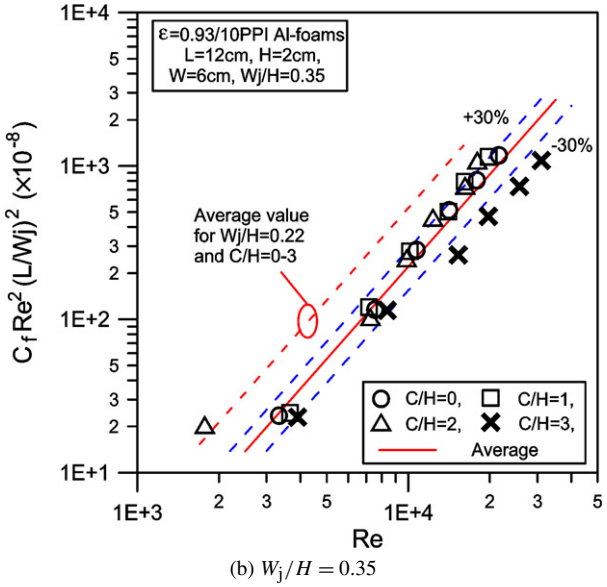


(b) $W_j/H = 0.35$

Fig. 7. Dimensionless pressure drop as a function of jet Reynolds number.

Wadsworth and Mudawar [1] examined the fluid FC-72 slot jet impinging cooling without a porous block and yielded the correlation for the average Nusselt number as

$$Nu/Pr^{1/3} = 3.06Re_D^{0.5} + 0.099Re_D^{0.664}\left[(L - W_j)/W_j\right]^{0.664} \quad (9)$$

where $Re_D$ is defined as $\rho_f V_j D_h/\mu$ and $D_h$ is the hydraulic diameter of the slot nozzle. The scope of application is $H/W_j =$

1–20, $(L - W_j)/W_j = 24$–$99$ and $Re_D = 1000$–$30\,000$. Plotting Eq. (9) in Fig. 4 reveals that $Nu$ with the aluminum foam block was 3–5 times as large as that without the aluminum foam block. Therefore, the impinging cooling performance can be effectively improved by applying the metallic porous block.

Fig. 5 shows the effects $Re$, $W_j/H$ and $C/H$ on the dimensionless wall temperatures ($\theta_w$) along the channel axis (as shown in Fig. 3(b)). In this investigation, the inverter adjusted the frequency of alternating current to control the rotational speed of the blower's motor, then the various air flow rate could be blown from the blower. Six frequencies, 10, 20, 30, 40, 50 and 60 Hz, were used. The systems with various $W_j/H$ and $C/H$ yield various $Re$ values at a given frequency. Fig. 5 reveals that all of the $\theta_w$ distributions were similar. The $\theta_w$ at the stagnation point ($x/L = 0$) under the slot jet flow was minimal, and monotonously rise along the channel axis until the channel exit. The uniformity of dimensionless temperatures can be examined by the parameter $(\theta_{w,max.} - \theta_{w,min.})/\bar{\theta}_w$. It can be found that the value of $(\theta_{w,max.} - \theta_{w,min.})/\bar{\theta}_w$ was larger than 0.25, suggesting an obvious change in $\theta_w$. Also, $\theta_w$ decreases as $Re$ increases, $\theta_w$ increases slightly as $C/H$ increases, however, $W_j/H$ increased from 0.22 to 0.35 (59% increase), and the change of $\theta_w$ could be neglected, heat transfer reduces as $\theta_w$ increases, thus, the effects of $Re$, $W_j/H$ and $C/H$ on $\theta_w$ could reflect the effects of relevant parameters on heat transfer. In other words, $Nu$ increases as $Re$ increases, $Nu$ decreases slightly as $C/H$ increases, $W_j/H$ has no effect on $Nu$, all $Nu$ values as a function of $Re$ are shown in Fig. 6. Based on the experimental results shown in Fig. 6, a correlation between the Nusselt and Reynolds numbers for each case is obtained by a least-square fitting method. The correlation is expressed in term of the following equation

$$Nu = m_1 Re^{n_1} \tag{10}$$

The coefficients, $m_1$ and $n_1$, of Eq. (10) are tabulated in Table 2. Table 2 also shows the range of application and the standard error of estimate for each case. The result shows that the fit is in good agreement with measured $Nu$. Notably, when $W_j/H = 1.24$ and $C/H \geqslant 1$, the downstream flow field of the porous block could become complicated and unstable. Factors including flow recirculation, flow reattachment and separation, could lead to unpredictable values of flow velocity and pressure drop, thus, there were no data under this parameter range.

Fig. 7 displays effects of $Re$, $W_j/H$ and $C/H$ on the dimensionless pressure drop ($C_f Re^2 (L/W_j)^2$). The experimental data indicate that the value of $C_f Re^2 (L/W_j)^2$ increased as $Re$ increased. Besides, the value of $C_f Re^2 (L/W_j)^2$ increased as $W_j/H$ decreased when the $Re$ and $C/H$ were specified. This relationship can be explained as follows. The pressure drop in the present system has two main causes. One is the slot jet nozzle; the other is the aluminum foam block. At a particular $Re$, a large $W_j/H$ is responsible for a small jet flow velocity, suggesting small pressure drops in both the slot jet nozzle and the perpendicular flow regions of the porous block. Finally, the effect of $C/H$ on the dimensionless pressure drop ($C_f Re^2 (L/W_j)^2$) seemed irregular, but the $C_f Re^2 (L/W_j)^2$ under different $C/H$ values distributed almost within the range of $\pm 30\%$. Based on the experimental results shown in Fig. 7, a correlation between

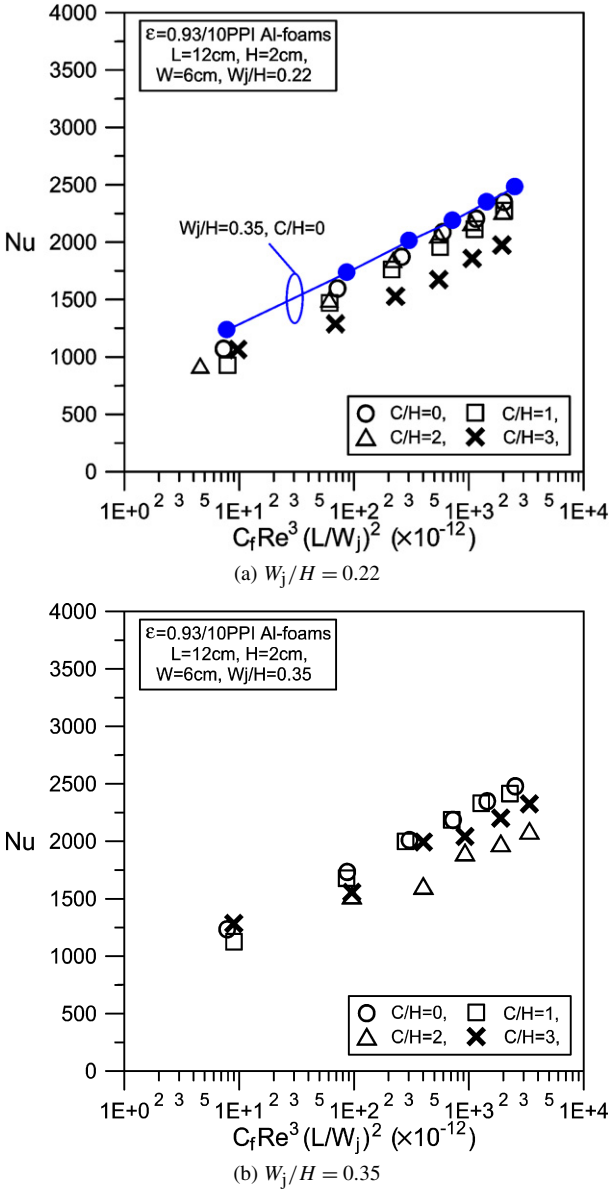


(a) $W_j/H = 0.22$

(b) $W_j/H = 0.35$

Fig. 8. Nusselt number as a function of dimensionless pumping power.

$C_f Re^2 (L/W_j)^2$ and $Re$ is expressed in term of the following equation

$$C_f Re^2 (L/W_j)^2 = m_2 Re^{n_2} \tag{11}$$

The coefficients ($m_2$ and $n_2$), the range of application and the standard error of estimate for each case are listed in Table 3.

Attention is now turned to the pumping power constraint. For systems with various $W_j/H$ and $C/H$, a fixed pumping power can yield various rates of flow of the air used to cool the heated surface. A parameter, $C_f Re^3 (L/W_j)^2$, was introduced as the dimensionless pumping power. Fig. 8 plots the average Nusselt number ($Nu$) against $C_f Re^3 (L/W_j)^2$. The data depict that the $Nu$ increased with $C_f Re^3 (L/W_j)^2$ for systems with various $W_j/H$ and $C/H$. The $Nu$ in the configuration without by-pass flow (i.e. $C/H = 0$) generally exceeded that with by-pass flow (i.e. $C/H = 1$–$3$) at a given pumping power. Within the successfully measured parameter ($W_j/H = 0.22$–$0.35$, $C/H =$

Table 3
Coefficients of the correlations between $C_f Re^2 (L/W_j)^2$ and $Re$

| $\varepsilon = 0.93/10$ *PPI* Al-foams $L \times W \times H$ cm $= 12 \times 6 \times 2$ | | $C_f Re^2 (L/W_j)^2 = m_2 Re^{n_2}$ | | | |
|---|---|---|---|---|---|
| $W_j/H$ | $C/H$ | $Re$ | $m_2$ | $n_2$ | Standard error |
| 0.22 | 0 | 2710–15 973 | 76.221 | 2.193 | 0.248E–2 |
| 0.22 | 1 | 2596–15 772 | 482.74 | 2.019 | 3.320E–2 |
| 0.22 | 2 | 1697–15 760 | 5384.7 | 1.749 | 1.685E–2 |
| 0.22 | 3 | 3262–15 524 | 16.719 | 2.374 | 3.345E–2 |
| 0.35 | 0 | 3333–21 622 | 77.999 | 2.119 | 0.427E–2 |
| 0.35 | 1 | 3657–19 825 | 19.518 | 2.277 | 0.438E–2 |
| 0.35 | 2 | 1774–17 993 | 5348.0 | 1.688 | 11.34E–2 |
| 0.35 | 3 | 3903–31 003 | 738.98 | 1.816 | 1.087E–2 |

0–3 and $Re = 1697$–$31\,003$), under the same dimensionless pumping power, the optimal cooling performance appeared on $W_j/H = 0.35$ and $C/H = 0$.

## 4. Conclusions

This investigation experimentally studied the convective heat transfer and pressure drop in metallic porous block with a confined slot jet. Aluminum foam block with $\varepsilon = 0.93/10$ *PPI* and was employed. The coolant was air. The results reveal that Nusselt number with the aluminum foam block was 3–5 times as large as that without the aluminum foam block, suggesting a significant heat transfer enhancement in the impinging cooling system due to the metallic porous block. The effects of the ratio of the jet nozzle width to the porous block height ($W_j/H$), the ratio of the jet-to-foam tip distance to the porous block height ($C/H$) and the jet Reynolds number ($Re$) were also investigated. Within the successfully measured parameter ($W_j/H = 0.22$–$0.35$, $C/H = 0$–$3$ and $Re = 1697$–$31\,003$), the largest Nusselt number under a given dimensionless pumping power appeared on $W_j/H = 0.35$ and $C/H = 0$.

## Acknowledgement

The authors would like to thank the National Science Council of the Republic of China for financially supporting this research under Contract No. NSC 95-2221-E-344-004.

## References

[1] D.C. Wadsworth, I. Mudawar, Cooling of a multichip electronic module by mean of confined two-dimensional jets of dielectric liquid, ASME Journal of Heat Transfer 112 (1990) 891–898.
[2] K. Jambunathan, E. Lai, M.A. Moss, B.L. Button, A review of heat transfer data for single circular jet impingement, International Journal of Heat and Fluid Flow 13 (2) (1992) 106–115.
[3] D.J. Womac, S. Ramadhyani, F.P. Incropera, Correlating equations for impingement cooling of small heat sources with single circular liquid jets, Journal of Heat Transfer 115 (1993) 106–115.
[4] D. Lytle, B.W. Webb, Air jet impingement heat transfer at low nozzle-plate spacings, International Journal of Heat and Mass Transfer 37 (12) (1994) 1687–1697.
[5] J.Y. San, C.H. Huang, M.H. Shu, Impingement cooling of a confined circular air jet, International Journal of Heat and Mass Transfer 40 (6) (1997) 1355–1364.
[6] M. Behnia, S. Parneix, Y. Shabany, P.A. Durbin, Numerical study of turbulent heat transfer in confined and unconfined impinging jets, International Journal of Heat and Fluid Flow 20 (1999) 1–9.
[7] E.M. Sparrow, A.P. Suopys, M.A. Ansari, Effect of inlet, exit, and fin geometry on pin fins situated in a turning flow, International Journal of Heat and Mass Transfer 27 (7) (1984) 1039–1054.
[8] L.G. Hansen, B.W. Webb, Air jet impingement heat transfer from modified surfaces, International Journal of Heat and Mass Transfer 36 (4) (1993) 989–997.
[9] G. Ledezma, A.M. Morega, A. Bejan, Optimal spacing between pin fins with impinging flow, ASME Journal of Heat Transfer 118 (1996) 570–577.
[10] L.A. Brignoni, S.V. Garimella, Experimental optimization of confined air jet impingement on a pin fin heat sink, IEEE Transactions on Components and Packaging Technology 22 (3) (1999) 399–404.
[11] Y. Kondo, H. Matsushima, T. Komatsu, Optimization of pin-fin heat sinks for impingement cooling of electronic packages, ASME Journal of Electronic Packaging 122 (2000) 240–246.
[12] J.G. Maveety, H.H. Jung, Heat transfer from square pin-fin heat sinks using air impingement cooling, IEEE Transactions Components and Packaging Technologies 25 (3) (2002) 459–469.
[13] J.S. Issa, A. Ortega, Experimental measurements of the flow and heat transfer of a square jet impinging on an array of square pin fins, ASME Journal of Electronic Packaging 128 (2006) 61–70.
[14] T.W. Lin, M.C. Wu, L.K. Liu, C.J. Fang, Y.H. Hung, Cooling performance of using a confined slot jet impinging onto heated heat sinks, ASME Journal of Electronic Packaging 128 (2006) 82–91.
[15] M.L. Hunt, C.L. Tien, Effects of thermal dispersion on forced convection in fibrous media, International Journal of Heat Mass Transfer 31 (1988) 301–309.
[16] V.V. Calmidi, R.L. Mahajan, Forced convection in high porosity metal foams, ASME Journal of Heat Transfer 122 (2000) 557–565.
[17] S.Y. Kim, B.H. Kang, J.H. Kim, Forced convection from aluminum foam materials in an asymmetrically heated channel, International Journal of Heat Mass Transfer 44 (2001) 1451–1454.
[18] D. Angirasa, Experimental investigation of forced convection heat transfer augmentation with metallic fibrous materials, International Journal of Heat Mass Transfer 45 (2002) 919–922.
[19] D. Angirasa, Forced convective heat transfer in metallic fibrous materials, ASME Journal of Heat Transfer 124 (2002) 739–745.
[20] K.C. Leong, L.W. Jin, An experimental study of heat transfer in oscillating flow through a channel filled with an aluminum foam, International Journal of Heat Mass Transfer 48 (2005) 243–253.
[21] W.S. Fu, H.C. Huang, Thermal performances of different shape porous blocks under an impinging jet, International Journal of Heat Mass Transfer 40 (1997) 2261–2272.
[22] H. Hadim, M. North, Forced convection in a sintered porous channel with inlet and outlet slots, International Journal of Thermal Sciences 44 (2005) 33–42.
[23] T.M. Jeng, S.C. Tzeng, Numerical study of confined slot jet impinging on porous metallic foam heat sink, International Journal of Heat Mass Transfer 48 (2005) 4685–4694.

[24] N.H. Saeid, A.A. Mohamad, Jet impingement cooling of a horizontal surface in a confined porous medium: Mixed convection regime, International Journal of Heat Mass Transfer 49 (2006) 3906–3913.
[25] V.V. Calmidi, R.L. Mahajan, The effective thermal conductivity of high porosity fibrous metal foams, ASME Journal of Heat Transfer 121 (1999) 466–471.
[26] D.A. Nield, Estimation of the stagnant thermal conductivity of saturated porous media, International Journal of Heat Mass Transfer 34 (1991) 1575–1576.
[27] S.J. Kline, F.A. McClintock, Describing uncertainties in single-sample experiments, Mechanical Engineering (1953) 3–8.
[28] R.J. Moffat, Contributions to the theory of single-sample uncertainty analysis, ASME Journal of Fluids Engineering 104 (1986) 250–260.
[29] S.C. Tzeng, T.M. Jeng, Convective heat transfer in porous channels with 90-deg turned flow, International Journal of Heat Mass Transfer 49 (2006) 1452–1461.
[30] W.H. Shih, W.C. Chiu, W.H. Hsieh, Height effect on heat-transfer characteristics of aluminum-foam heat sinks, ASME Journal of Heat Transfer 128 (2006) 530–537.